Coherent instabilities in random lasers

Jonathan Andreasen, Patrick Sebbah, and Christian Vanneste
Laboratoire de Physique de la Matière Condensée, CNRS UMR 6622, Université de Nice-Sophia Antipolis, Parc Valrose, F-06108, Nice Cedex 02, France
(Received 25 November 2010; published 16 August 2011)

A numerical study is presented of random lasers as a function of the pumping rate above the threshold for lasing. Depending on the leakiness of the system resonances, which is typically larger in random lasers compared to conventional lasers, we observe that the stationary lasing regime becomes unstable above a second threshold. Coherent instabilities are observed as self pulsation at a single frequency of the output intensity, population inversion, as well as the atomic polarization. We find these Rabi oscillations have the same frequency everywhere in the random laser despite the fact that the field intensity strongly depends on the spatial location.

DOI: 10.1103/PhysRevA.84.023826 PACS number(s): 42.55.Zz, 42.65.Sf, 05.45.−a

I. INTRODUCTION

Since their prediction by Lethokov [1], random lasers have been the subject of numerous studies. After the first experiments at the end of the '80s [2], the observation of narrow lines in the laser spectra [3–5] led to a several-years debate about the nature of the lasing modes. Compared to conventional lasers, random lasers are typically very open (leaky) and do not make use of a traditional resonator or cavity. Important progress has been recently made in theoretical and numerical studies that discuss the correspondence between lasing modes and resonances of the passive system without gain [6–12]. Contrastingly, the interaction of lasing modes in the multimode regime of a random laser is not so well known. Experimentally, the multimode response of random lasers using picosecond optical pumping has been studied at the beginning of the 2000s [13–15]. These random lasers are in a transient regime rather than a steady regime, thus complicating analysis of mode competition. Numerically, time-domain simulations [16] have shown quantitative agreement with experiments but concern the limiting case of a broad laser spectrum in the highly multimode regime. Theoretically, only recently the *ab initio* laser theory [10] was able to make analytical predictions about the multimode lasing spectrum above threshold when mode competition takes place. Devoted to a random laser under steady pumping, it relies on the assumption that the atomic population inversion is time-independent and that there exists a steady-state multiperiodic solution of the laser field and polarization of the atomic medium. An important issue remains unaddressed: a stationary regime may not always exist under steady pumping of a random laser. Though different kinds of nonstationary regimes and instabilities are known to take place in conventional lasers, they have never been reported in random lasers.

Coherent instabilities in homogeneously broadened lasers [17], i.e., pulsed emission that involves not only the field intensity and atomic populations but also the atomic polarization, are known to take place in conventional lasers. In particular, the single-mode Lorenz-Haken (LH) [18,19] and multimode Risken-Nummedal-Graham-Haken (RNGH) [20,21] instabilities have been extensively studied since the end of the '60s. However, experimental evidence of these effects is not only scarce but also a matter of debate [22], due to the difficulty in finding laser systems in the required parameter range. Moreover, investigation of these instabilities has been mainly carried out when the field and atomic variables are essentially spatially uniform [17]. Hence, the nature of such instabilities in highly nonuniform systems such as random lasers are open questions. Such questions are reminiscent of those related to the nature of secondary instabilities that are observed, for instance, in nonuniform nonlinear hydrodynamic systems [23] or related to the synchronization of nonidentical oscillators [24].

In this paper, we numerically investigate one-dimensional (1D) and two-dimensional (2D) random lasers using steady external pumping by progressively increasing the pumping rate. After observing stationary single-mode lasing and multimode lasing, we find that the stationary regime can become unstable for sufficiently large values of the pumping rate. It appears as time oscillations of the output intensity, atomic population inversion, and atomic *polarization*. It is found to be related to Rabi oscillations and of the same type as instabilities discovered earlier in conventional lasers [19–21]. However, the fundamental difference here in random lasers is that the internal field intensity strongly fluctuates as a function of position. This specific feature of random lasers prevents us from defining a unique Rabi oscillation frequency in the system. Nonetheless, we observe that the oscillations have the same frequency at any point in the system, whatever the value of the local field intensity.

II. RANDOM STRUCTURES AND METHOD

The 1D random structures we consider are composed of 41 layers. Dielectric material with optical index $n_1 = 1.25$ separated by air gaps ($n_2 = 1$) results in a spatially modulated index $n(x)$. Outside the random medium, the index is 1. The system is randomized by specifying thicknesses for each layer as $d_{1,2} = \langle d_{1,2}\rangle(1 + \eta\zeta)$, where $\langle d_1\rangle = 100$ nm and $\langle d_2\rangle = 200$ nm are the average thicknesses of the layers, $\eta = 0.9$ represents the degree of randomness, and ζ is a random number in $(-1,1)$. The length of the random structure L is normalized to $\langle L\rangle = 6.1\ \mu$m. These parameters give a localization length $\xi \approx 11\ \mu$m.

The 2D random structures we consider are of size $L^2 = 1.1 \times 1.1\ \mu\text{m}^2$. They are made of circular dielectric particles with radius $r = 60$ nm, optical index $n_1 = 1.5$, and surface filling fraction $\Phi = 40\%$, which are randomly

distributed in a background medium of index $n_2 = 1$. Outside the random medium, the index is 1. The scattering mean free path $\ell_s \approx 0.3\ \mu$m and the localization length $\xi \approx 5\ \mu$m. The system is in the weakly scattering regime-intermediate between ballistic and diffusive.

The background medium (air) is chosen as the active part of the system and is modeled as a four-level atomic medium. We describe the time evolution of the fields by Maxwell's equations including a polarization term due to the atomic population inversion. Maxwell's equations are solved using the finite-difference time-domain method and C-PML absorbing boundary conditions in order to model the open system [25]. The corresponding equations are identical to those used in Ref. [26], where $T_1 = 100$ ps and $T_2 = 20$ fs so that the gain curve centered at $\lambda_a = 446.9$ nm has a spectral width $\Delta\lambda_a = 11$ nm. The control parameter is the pumping rate P_r at which an external mechanism transfers the atoms from the ground-state level 0 to the upper level 3 of the four-level system.

III. RESULTS

Figure 1 shows the emission spectra $|E(\lambda)|^2$ from a 2D random laser with increasing pumping rates. Just above the lasing threshold at $P_r = 2.50\ \text{ns}^{-1}$, a single lasing peak is observed in the emission spectrum [Fig. 1(a)]. The lasing wavelength $\lambda = 448.2$ nm is close to but not coincident with the gain center wavelength λ_a. This is indicative of lasing associated with a resonance of the random system [12]. The multimode regime is reached by $P_r = 3.00\ \text{ns}^{-1}$, with a second lasing peak appearing at $\lambda = 444.6$ nm [Fig. 1(b)]. With the pumping rate increased to $P_r = 13.0\ \text{ns}^{-1}$ [Fig. 1(c)], a large number of fine spectral features appears while the original lasing peaks are still observed. Such behavior persists for higher pumping rates with the frequency spacing between the fine spectral features increasing [Fig. 1(d) where $P_r = 20.0\ \text{ns}^{-1}$]. We studied ten different 2D random systems of the same size and found instabilities in all cases.

Since the same behavior is observed in 1D random lasers as exemplified by Fig. 2, and since analysis is simpler, we switch to 1D systems. Figure 2 shows the emission spectra $|E(\lambda)|^2$ from a 1D random laser with increasing pumping rates. Just above the lasing threshold at $P_r = 0.24\ \text{ns}^{-1} \equiv P_{\text{th}}$,

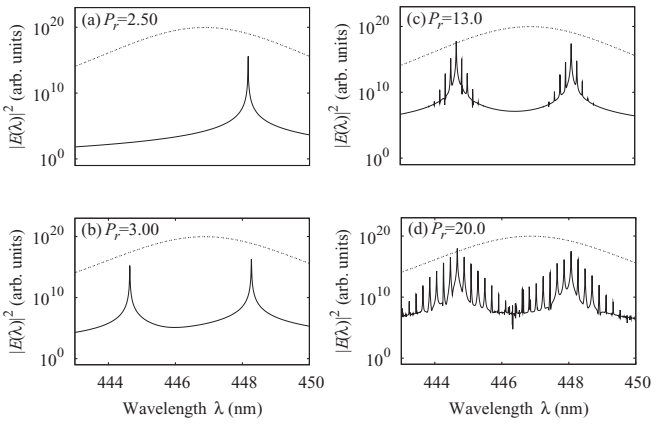

FIG. 1. Emission spectra $|E(\lambda)|^2$ for a 2D random system. The values of the pumping rate P_r are written in each panel in units ns^{-1}. The gain curve (dotted line) is overlaid.

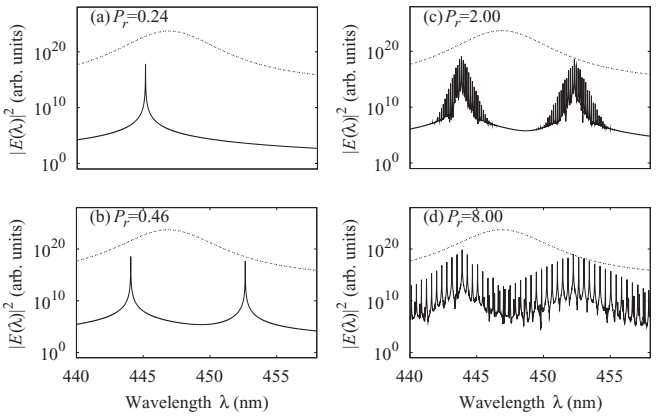

FIG. 2. Emission spectra $|E(\lambda)|^2$ for a 1D random system. The values of the pumping rate P_r are written in each panel in units ns^{-1}. The gain curve (dotted line) is overlaid.

a single lasing peak is observed in the emission spectrum [Fig. 2(a)]. The lasing wavelength $\lambda = 445.12$ nm is close to but not coincident with the gain center wavelength $\lambda_a = 446.90$ nm. We verified this lasing mode's association with a resonance of the random system [27] by comparing their intensity distributions (examples of lasing modes in 1D weakly scattering random lasers can be found in [11]). The multimode regime is reached by $P_r = 0.46\ \text{ns}^{-1}$, with a second lasing peak appearing at $\lambda = 452.64$ nm [Fig. 2(b)]. The second lasing mode is associated with a second resonance (verified by comparisons of intensity distributions). In all cases checked, the lasing mode corresponds essentially to only one resonance.

With the pumping rate increased to $P_r = 2.00\ \text{ns}^{-1}$ [Fig. 2(c)], numerous sidebands are generated on either side of the two lasing wavelengths. Such behavior persists for higher pumping rates, but the frequency spacing between the fine spectral features increases [Fig. 2(d), where $P_r = 8.00\ \text{ns}^{-1}$]. We emphasize that the sideband peaks cannot correspond to system resonances because their frequency spacing is much smaller than the intermode spacing shown clearly in Fig. 2(b). We studied ten different 1D random systems and when they became unstable, we found the same spectral behavior.

To investigate the cause of this spectral behavior, we examine the dynamics of the system. The output intensity $|E(t)|^2$ is measured on one side of the random system and averaged over each optical period T_a. The population inversion ΔN is averaged spatially:

$$\Delta N(t) = \int_0^{\tilde{L}} [N_2(x,t) - N_1(x,t)]\, dx/(\tilde{L} N_a), \qquad (1)$$

where N_a is the total density of atoms and the integration is over the gain domain $\tilde{L}$. The fluctuations of the population inversion are measured as the temporal standard deviation:

$$\sigma^2 = \int_{t_1}^{t_2} [\Delta N(t) - \langle \Delta N(t) \rangle]^2\, dt/(t_2 - t_1). \qquad (2)$$

Dynamic behavior of the output intensity and population inversion for the smallest pumping rate at which the spectral splitting occurs $P_r = 0.48\ \text{ns}^{-1}$ (2 times the lasing threshold) is shown in Fig. 3(a). The population inversion clearly oscillates resulting in a series of optical pulses. First, we stress that this

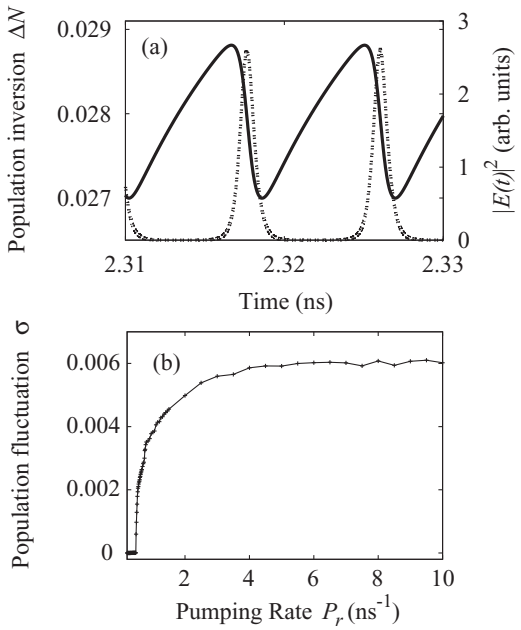

FIG. 3. (a) Population inversion (solid line) and intensity $|E(t)|^2$ (dotted line) for a 1D random system with $P_r = 0.48$ ns^{-1}. (b) Temporal standard deviation σ of the population inversion vs. pumping rate P_r.

behavior occurs in a time interval late in the simulation, chosen to avoid the transient regime where relaxation oscillations take place and decay with a decay time $\tau_{\rm ro} \approx 100$ ps. Unlike relaxation oscillations, where the atomic polarization does not play a role [28], we find these oscillations to be coherent in nature since the polarization of the gain medium also oscillates at the same frequency as the population inversion and intensity.

Below the instability threshold, in the multimode regime, the polarization and population inversion also fluctuate in time due to mode beating. However, these fluctuations are small. In contrast, at these larger pumping rates, temporal oscillations increase dramatically putting the system in a highly nonstationary regime. Figure 3(b) shows the temporal standard deviation σ of $\Delta N(t)$ with increasing P_r. In this case, σ increases by 2 orders of magnitude from $P_r = 0.47$ to 0.48 ns^{-1} and keeps increasing until $P_r = 4.00$ ns^{-1}.

Spectral behavior of laser emission in a smaller frequency range is shown in Figs. 4(a) and 4(b). A frequency comb is evident with regularly spaced peaks. The frequency spacing between peaks increases from $\Delta\omega = 1.8$ to 3.4 THz as the pumping rate increases from $P_r = 4.00$ to 8.00 ns^{-1}. Figures 4(c) and 4(d) show the population inversion spectrum $\Delta N(\omega)$ [calculated from $\Delta N(t)$ in Eq. (1)]. The first and largest nonzero peaks in $\Delta N(\omega)$ for the two pumping rates are at $\omega_N = 1.8$ and 3.4 THz. Thus, ω_N corresponds precisely to the frequency spacing $\Delta\omega$ of the laser emission for both pumping rates. We verified that these two values equal each other for intermediate pumping rates as well. The additional higher-frequency peaks in $\Delta N(\omega)$ are harmonics related to the sharp sawtooth behavior of $\Delta N(t)$ seen in Fig. 3(a).

With the same oscillatory behavior observed in the atomic polarization, population inversion, and field intensity, we investigate the relation to Rabi oscillations. In a random laser,

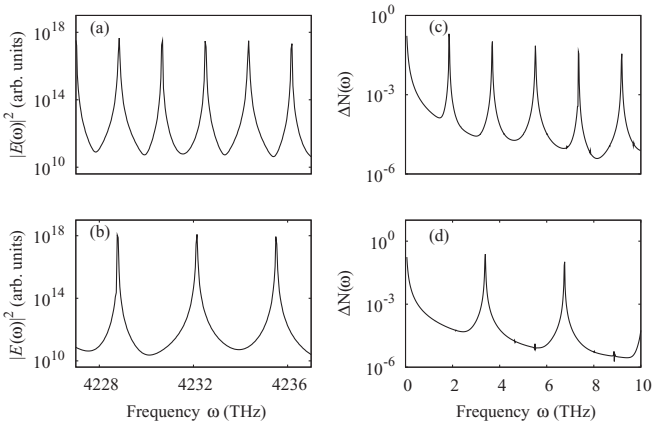

FIG. 4. Emission spectra $|E(\omega)|^2$ (a,b) and population inversion $\Delta N(\omega)$ (c,d) with $P_r = 4.00$ ns^{-1} (a,c) and $P_r = 8.00$ ns^{-1} (b,d) for a 1D random system. ω_N is the smallest (nonzero) frequency peak in $\Delta N(\omega)$ and corresponds to the frequency spacing in the emission spectrum.

the Rabi frequency Ω is not a well-defined quantity since the field amplitude not only varies temporally but also spatially. There is precedent [29] for temporal averaging of the field to estimate Ω, but effects due to spatial variations of the field remain largely unexplored in this context. One striking result, as demonstrated in Fig. 5(a), is that the frequency of the coherent oscillations does not depend on the spatial location within the system. For example, the field intensity at $x = 5.2\,\mu$m in Fig. 5(a) is more than an order of magnitude smaller than at the other two locations while the oscillation frequency in all cases is the same. The local field intensity $I(x)$ can be used to calculate a local Rabi frequency as $\Omega_L = \gamma I^{1/2}(x)/\hbar$, where $\gamma = \sqrt{3\lambda_a^3\hbar\epsilon_0/8\pi^2 T_1} = 1.8 \times 10^{-28}$ C m is the atomic dipole coupling term. According to the local intensities, $\Omega_L(x = 0.2\ \mu\text{m}) = 6.9$ THz, $\Omega_L(x = 2.1\ \mu\text{m}) = 4.8$ THz, and $\Omega_L(x = 5.2\ \mu\text{m}) = 0.4$ THz. We observe the same behavior in 2D as indicated by Fig. 5(b). Eleven different sampling locations yield local Rabi frequencies ranging from 0.55 to 2.5 THz. The polarization, however, reveals a frequency of 1.6 THz, matching the splitting frequency in Fig. 1(c). This frequency of the coherent oscillations at the same sampling locations is identical as that shown by the multiple polarization spectra in Fig. 5(b). This is contrary to expected behavior since the standard Rabi frequency should be proportional to the local field amplitude and thus, vary strongly with position.

In order to relate the observed single oscillation frequency in the random laser to an effective Rabi frequency, we consider the following. For a fixed pumping rate, all quantities averaged over space and long times (compared to $1/\Omega$) become nearly constant eventually. Focusing on a late temporal region after the transient regime, we calculate the spatiotemporally averaged internal field intensity I_a and estimate the Rabi frequency as

$$\Omega = \gamma I_a^{1/2}/\hbar. \tag{3}$$

Figure 6 compares ω_N to Ω for a 1D and 2D random system. We find the same trend for a wide range of pumping rates (from 2–40 times the lasing threshold). The quantitative difference between ω_N and Ω changes from realization to realization

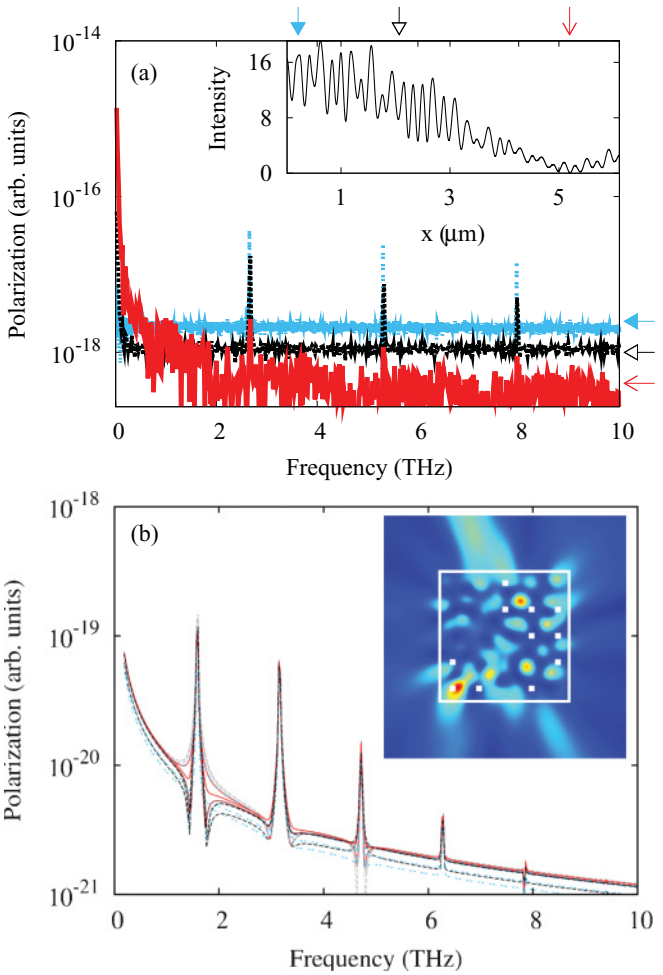

FIG. 5. (Color online) Atomic polarization spectra at different spatial locations for (a) 1D random system with $P_r = 6.00\ \mathrm{ns}^{-1}$ and (b) 2D random system with $P_r = 13.0\ \mathrm{ns}^{-1}$. (Insets) Time-averaged spatial intensity distributions marking (a) 3 sampling locations and (b) 11 sampling locations. All locations yield the same low oscillation frequency in both cases.

because the precise value of the intensity to use in Eq. (3) is unknown. The important behavior here is that ω_N scales as the square root of the intensity. This shows the population inversion and atomic polarization oscillations (which induce spectral field sidebands) are similar to Rabi oscillations.

For the 1D resonances associated with the two lasing modes in Fig. 2, the lifetimes measured [27] from the passive system are $\tau = 11$ fs and $\tau = 16$ fs, respectively. Hence, the 1D open random laser considered here is in the so-called bad-cavity limit, where the mode lifetime $\tau < (1/T_1 + 1/T_2)^{-1}$. In this limit, the LH instability manifests itself in sideband peaks around the lasing peak, resulting from gain provided by Rabi oscillations. This is the behavior observed in Fig. 4. Another condition on such instabilities is that the Rabi frequency must be greater than the inverse atomic relaxation times so the coherent oscillations are not destroyed. This means the intensity and therefore the pumping rate must be sufficiently large. The instability threshold observed here is roughly twice the lasing threshold. Many elements may contribute to the precise threshold value. It ranges from 1–9 P_{th} in

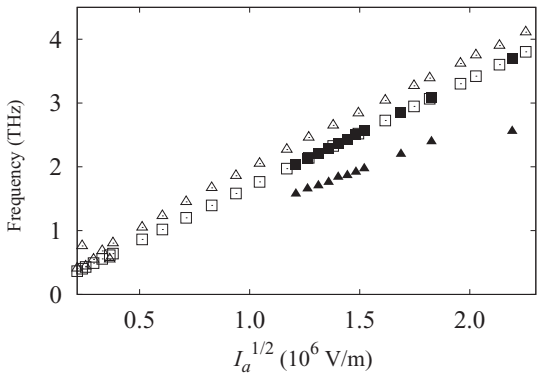

FIG. 6. Estimated Rabi frequency Ω (squares) and the population inversion frequency ω_N (triangles) for 1D (open symbols) and 2D (solid symbols) random systems vs. the internal field $I_a^{1/2}$.

previous works, due to such factors as the laser model (two-, three-, four-level) [30], a saturable absorber [31,32], or spatial variations [33,34].

We examined the behavior of 30 realizations of random structures in 1D and 2D. Mode frequencies, lifetimes, and spatial intensity distributions change for each realization. Despite the differences from realization to realization, the same trend is found in 1D and 2D systems between $\Delta\omega$, ω_N, and Ω as in Fig. 6; i.e., they scale linearly with $I_a^{1/2}$. Furthermore, when the instability occurs, the condition on τ is always satisfied. Due to the small density of states, the results in these systems have all the characteristics of the single-mode LH instability as opposed to the multimode RNGH instability [35].

We have also studied larger 2D systems with a larger density of states. In such systems, we have not found a case in which the instability did not manifest itself. The random structures considered in this case are of size $L^2 = 5.0 \times 5.0\ \mu\mathrm{m}^2$. Though we could observe in a few such systems the instabilities described above, most systems exhibit an instability where the spectrum is complicated by the presence of many lasing and nonlinear

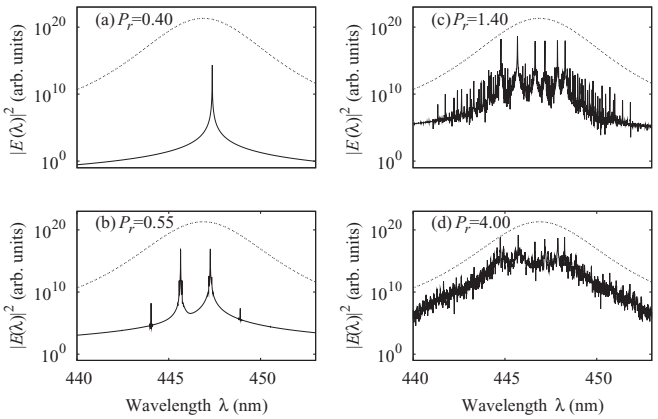

FIG. 7. Emission spectra $|E(\lambda)|^2$ for a large ($L^2 = 5.0 \times 5.0\ \mu\mathrm{m}^2$) 2D random system. The values of the pumping rate P_r are written in each panel in units ns^{-1}. The gain curve (dotted line) is overlaid. The two side peaks in (b) with smaller amplitudes (by 9 orders of magnitude) are due to four-wave mixing.

wave-mixing peaks [36], as illustrated by Fig. 7. Hence, it is difficult to distinguish between the multimode or single-mode instability as in 1D or small 2D systems.

IV. CONCLUSION

When increasing the pumping rate above the lasing threshold, we found that the stationary regime of random lasers is not stable and gives rise to a coherent instability due to very short lifetimes of the system resonances. The bad-cavity limit, and hence the nonstationary regime, is likely to be reached in experiments because: (i) random lasers are open systems with strong leakage and (ii) atomic lifetimes are typically longer than those we used in this paper. One striking result is that the Rabi oscillations occur at a well-defined frequency everywhere in the random laser despite the fact that the field intensity strongly depends on the spatial location. After recent progress in the theoretical understanding of random lasers in the stationary regime [12], this work is a step toward understanding the rich physics of such lasers which combine random systems, complex light-matter interaction, and nonlinear dynamic behavior. These results raise new questions concerning our physical understanding of coherent instabilities in laser physics.

ACKNOWLEDGMENTS

We thank H. Cao, M. Giudici, G.-L. Lippi, and L. Gil for stimulating discussions. This work was supported by the ANR under Grant No. ANR-08-BLAN-0302-01, the PACA region, the CG06, and the Groupement de Recherche 3219 MesoImage. JA acknowledges support from the Embassy of France in the United States. This work was performed using HPC resources from GENCI-CINES (Grant No. 2010-99660).

[1] V. S. Letokhov, Sov. Phys. JETP **26**, 835 (1968).
[2] V. M. Markushev, V. F. Zolin, and C. M. Briskina, Zh. Prikl. Spektrosk. **45**, 847 (1986).
[3] H. Cao, Y. G. Zhao, H. C. Ong, S. T. Ho, J. Y. Dai, J. Y. Wu, and R. P. H. Chang, Appl. Phys. Lett. **73**, 3656 (1998).
[4] H. Cao, Y. G. Zhao, S. T. Ho, E. W. Seelig, Q. H. Wang, and R. P. H. Chang, Phys. Rev. Lett. **82**, 2278 (1999).
[5] S. V. Frolov, Z. V. Vardeny, K. Yoshino, A. Zakhidov, and R. H. Baughman, Phys. Rev. B **59**, R5284 (1999).
[6] C. Vanneste and P. Sebbah, Phys. Rev. Lett. **87**, 183903 (2001).
[7] X. Jiang and C. M. Soukoulis, Phys. Rev. E **65**, 025601 (2002).
[8] C. Vanneste, P. Sebbah, and H. Cao, Phys. Rev. Lett. **98**, 143902 (2007).
[9] H. E. Türeci, L. Ge, S. Rotter, and A. D. Stone, Science **320**, 643 (2008).
[10] H. E. Türeci, A. D. Stone, L. Ge, S. Rotter, and R. J. Tandy, Nonlinearity **22**, C1 (2009).
[11] J. Andreasen, C. Vanneste, L. Ge, and H. Cao, Phys. Rev. A **81**, 043818 (2010).
[12] J. Andreasen, A. Asatryan, L. Botten, M. Byrne, H. Cao, L. Ge, L. Labonté, P. Sebbah, A. D. Stone, H. E. Türeci *et al.*, Adv. Opt. Photon. **3**, 88 (2011).
[13] C. M. Soukoulis, X. Jiang, J. Y. Xu, and H. Cao, Phys. Rev. B **65**, 041103(R) (2002).
[14] H. Cao, X. Jiang, Y. Ling, J. Y. Xu, and C. M. Soukoulis, Phys. Rev. B **67**, 161101(R) (2003).
[15] X. Jiang, S. Feng, C. M. Soukoulis, J. Zi, J. D. Joannopoulos, and H. Cao, Phys. Rev. B **69**, 104202 (2004).
[16] C. Conti, M. Leonetti, A. Fratalocchi, L. Angelani, and G. Ruocco, Phys. Rev. Lett. **101**, 143901 (2008).
[17] L. M. Narducci and N. B. Abraham, *Laser Physics and Laser Instabilities* (World Scientific, Singapore, 1988).
[18] E. N. Lorenz, J. Atmos. Sci. **20**, 130 (1963).
[19] H. Haken, Phys. Lett. A **53**, 77 (1975).
[20] H. Risken and K. Nummedal, J. Appl. Phys. **39**, 4662 (1968).
[21] P. Graham and H. Haken, Z. Phys. **213**, 420 (1968).
[22] E. Roldán, G. J. de Valcárcel, F. Prati, F. Mitschke, and T. Voigt, in *Trends in Spatiotemporal Dynamics in Lasers. Instabilities, Polarization Dynamics, and Spatial Structures*, edited by O. Gomez-Calderon and J. M. Guerra (Research Signpost, Trivandrum, India, 2005), pp. 1–80.
[23] H. Riecke and H.-G. Paap, Phys. Rev. Lett. **59**, 2570 (1987), and references therein.
[24] A. S. Pikovsky, M. Rosenblum, and J. Kurths, *Synchronization: A Universal Concept in Nonlinear Sciences* (Cambridge University Press, Cambridge, 2001).
[25] A. Taflove and S. Hagness, *Computational Electrodynamics* (Artech House, Boston, 2005), 3rd ed.
[26] P. Sebbah and C. Vanneste, Phys. Rev. B **66**, 144202 (2002).
[27] M. Born and E. Wolf, *Principles of Optics* (Pergamon Press, New York, 1975), we used the transfer matrix method to find resonances in 1D.
[28] A. E. Siegman, *Lasers* (University Science Books, Mill Valley, 1986).
[29] L. W. Hillman, J. Krasinski, K. Koch, and J. C. R. Stroud, J. Opt. Soc. Am. B **2**, 211 (1985).
[30] E. M. Pessina, F. Prati, J. Redondo, E. Roldán, and G. J. de Valcárcel, Phys. Rev. A **60**, 2517 (1999).
[31] C. Y. Wang, L. Diehl, A. Gordon, C. Jirauschek, F. X. Kärtner, A. Belyanin, D. Bour, S. Corzine, G. Höfler, M. Troccoli *et al.*, Phys. Rev. A **75**, 031802(R) (2007).
[32] A. Gordon *et al.*, Phys. Rev. A **77**, 053804 (2008).
[33] J. F. Urchueguía, G. J. de Valcárcel, E. Roldán, and F. Prati, Phys. Rev. A **62**, 041801 (2000).
[34] F. Prati, E. M. Pessina, G. J. de Valcárcel, and E. Roldán, Opt. Commun. **185**, 153 (2000).
[35] Though in the multimode regime in Figs. 1 and 2, the lasing modes are well separated and observations at each lasing frequency are characteristic of the single-mode LH instability. For the multimode RNGH instability, the Rabi frequency is at least equal to the mode spacing.
[36] The presence of nonlinear wave-mixing in random systems is well known, e.g., S. E. Skipetrov, Nature **432**, 285 (2004), and references therein. Such mixing in the context of random lasing, however, is discussed further in a paper currently in preparation, see arXiv:1107.5990 [physics.optics].